

# Soft Matter

Accepted Manuscript



This is an *Accepted Manuscript*, which has been through the Royal Society of Chemistry peer review process and has been accepted for publication.

*Accepted Manuscripts* are published online shortly after acceptance, before technical editing, formatting and proof reading. Using this free service, authors can make their results available to the community, in citable form, before we publish the edited article. We will replace this *Accepted Manuscript* with the edited and formatted *Advance Article* as soon as it is available.

You can find more information about *Accepted Manuscripts* in the [Information for Authors](#).

Please note that technical editing may introduce minor changes to the text and/or graphics, which may alter content. The journal's standard [Terms & Conditions](#) and the [Ethical guidelines](#) still apply. In no event shall the Royal Society of Chemistry be held responsible for any errors or omissions in this *Accepted Manuscript* or any consequences arising from the use of any information it contains.



Journal Name

COMMUNICATION

## Switching wormlike micelles of selenium-containing surfactant using redox reaction

Received 00th January 20xx,  
Accepted 00th January 20xx

Yongmin Zhang,<sup>a\*</sup> Weiwei Kong,<sup>a</sup> Cheng Wang,<sup>a</sup> Pengyun An,<sup>a</sup> Yun Fang,<sup>a</sup> Zhirong Qin,<sup>c</sup> Yujun Feng,<sup>b\*</sup> and Xuefeng Liu<sup>a\*</sup>

DOI: 10.1039/x0xx00000x

www.rsc.org/

**A novel redox-switchable wormlike micellar system was developed based on selenium-containing zwitterionic surfactant and commercially available anionic surfactant sodium dodecyl sulfate, which reversibly and fast responds to H<sub>2</sub>O<sub>2</sub> and vitamin C, and shows circulatory gel/sol transition, reflecting changes in aggregate morphology from entangled worms to vesicles.**

A major scientific challenge of the past decade pertaining to the field of soft matter has been to craft stimuli-responsive “adaptable” materials, inspired by nature, which can dynamically alter their structures and functionalities on demand, in response to triggers produced by environmental changes.<sup>1</sup> Amongst these, smart switchable wormlike micelles (WLMs) represents a new avenue in the design of intelligent materials.<sup>2</sup> Reminiscent of polymer solutions, WLMs exhibit fascinating viscoelastic behaviour<sup>3</sup> and even form physical gel<sup>4</sup> at low concentration, because of the formation of 3D network from the low-molecular-weight surfactants, and the nanostructured micellar gels can be translated into low-viscosity Newtonian solutions by a stimulus, or vice versa. Such an intelligent “on” and “off” switchable modes hold great promise and enable the smart WLMs to find specialized applications ranging from oil and gas production, drag reduction, drug delivery, cleaning processes to bio mimicry.<sup>1–3</sup> The structural changes happening at the nanoscopic level, in turn, induce major changes of the macroscopic characteristics, affecting properties such as viscosity and elasticity, leading in some cases to an effective “sol/gel” transition.

The “switching” on and off of the smart WLMs has now been extensively reported using optical,<sup>5</sup> thermal,<sup>6</sup> CO<sub>2</sub>,<sup>7</sup> or pH triggers<sup>8</sup> and is now envisaged for other stimuli present in life process. Transition, though, control on the rheological properties of

surfactant solution using redox reaction has been rarely addressed. Among various external stimuli, redox is particularly intriguing for their promising applications in physiological environments, where the redox process is constantly and widely present.<sup>9</sup> Based on pathophysiological studies, inflammatory or tumor cells often generally owns a higher local redox potential than the healthy ones, implying it may be used to selectively trigger the viscoelasticity of WLMs within specific cells, leading to targeted drug release. To the best of our knowledge, however, there is only one example of redox-switchable WLMs system reported to date.<sup>10</sup> It was composed of a cationic ferrocenyl surfactant, (11-ferrocenylundecyl)trimethyl ammonium bromide (FTMA) and sodium salicylate. In reduced state, FTMA self-assemble into viscoelastic WLMs in the presence of sodium salicylate. When an electrolytic oxidation was performed on the sample for 24 h while the mixture was bubbled with N<sub>2</sub> and stirred, it turned into a low-viscosity short rodlike micellar solution. Because the very slow diffusion of electronic in viscoelastic worm solution, such a redox-responsive process is clearly time-consuming. Besides, the poor biocompatibility and strong irritancy of cationic ferrocenyl surfactant also restricts its further application in living organisms.<sup>9</sup> Thus, redox-induced WLMs based on a biocompatible surfactant with facile, fast and reversible responsiveness to local endogenous oxidants, such as reactive oxygen species, are highly desirable. To this end, we are interested in using a selenium-containing surfactant to construct redox-switchable WLMs since selenium is an essential microelement for human being<sup>9,11</sup> and possesses strong sensitivity to oxidative stimuli originating from its low binding energy.<sup>9,11</sup>

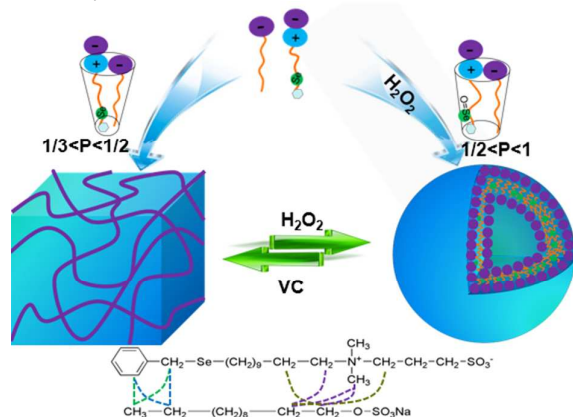
Herein, we demonstrated redox-switchable WLMs based on a mixture of synthetic selenium-containing zwitterionic surfactant, 3-(11-benzylselenanyl-undecyl)-dimethyl ammonium propane sulfonate (BSeUSBe, Scheme S1, and Figures. S1 to S8 in the Supporting Information) and commercially available anionic surfactant sodium dodecyl sulfate (SDS) (Scheme 1) in NaCl solution with precise stoichiometric ratio of 1:1 (referred as “BSeUSBe-SDS”). This system shows a fast redox-induced gel/sol reversible transition upon alternative addition of reactive oxygen species generated from hydrogen peroxide (H<sub>2</sub>O<sub>2</sub>) and vitamin C (VC), reflecting a smart transformation in morphology from WLMs to vesicles, which may

<sup>a</sup> Key Laboratory of Food Colloids and Biotechnology Ministry of Education, School of Chemical & Materials Engineering, Jiangnan University, 214122 Wuxi, People's Republic of China. E-mail: zhangym@jiangnan.edu.cn (Y. Zhang), xfliu@jiangnan.edu.cn (X. Liu)

<sup>b</sup> Polymer Research Institute, State Key Laboratory of Polymer Materials Engineering, Sichuan University, Chengdu 610065, PR China. E-mail: yifeng@scu.edu.cn (Y. Feng)

<sup>c</sup> Zhejiang Zanyu Technology Co. Ltd., Hangzhou, China  
Electronic Supplementary Information (ESI) available: [Experimental details, synthesis and additional results.]. See DOI: 10.1039/x0xx00000x

provide potential application as a smart gel in the fields of glutathione peroxidase (GPx) mimic.



**Scheme 1.** Redox-control reversible transition from wormlike micelles to vesicles in the mixture of selenium-containing zwitterionic surfactant and sodium dodecyl sulfate.

As exhibited in Figure 1, a transparent and homogeneous micellar gel (BSeUSBe-SDS) was immediately obtained when 50 mmol BSeUSBe and 50 mmol SDS were mixed in 1 L 50 mM NaCl aqueous solution at ambient temperature followed by mechanical agitation for several minutes. The formed micellar gel can withstand its own weight in a long timescale when tripped upside down. Steady-state rheological measurement of BSeUSBe-SDS (Figure 2a) shows an obvious Newtonian plateau at low shear rates accompanied by a shear-thinning behavior beyond a critical shear rate ( $0.02 \text{ s}^{-1}$ ), indicating the rearrangement of tangled worms under shear stress, i.e., the presence of wormlike micellar 3D network.<sup>3c,12</sup> If the Newtonian plateau is extrapolated to zero-shear rate, the zero-shear viscosity ( $\eta_0$ ) is obtained as high as 300 Pa·s. In the dynamic rheological spectra obtained by oscillatory-shear measurements (Figure S9), the storage modulus ( $G'$ ) for the 50 mM BSeUSBe-SDS solution is always exceeds the loss modulus ( $G''$ ) over the entire shear frequency, signifying the formation of surfactant gels other than typical worm.<sup>3b,13</sup> The plateau modulus ( $G_0$ , the storage modulus at high shear frequency), is as high as  $\sim 15.1 \text{ Pa}$  and the relaxation time is as long as  $\sim 19.8 \text{ s}$ . According to the model of the overlapping rods,<sup>14</sup> for the current system, the aggregation numbers of the rods were estimated to about 10000, composed of 5000 BSeUSBe and 5000 SDS. All these observations together confirm that the solution of BSeUSBe-SDS gives rise to WLMs at room temperature, and thus the viscoelasticity from the entangled network.

However, if equimolar  $\text{H}_2\text{O}_2$  was added to 20 mL 50 mM BSeUSBe-SDS aqueous solution, the viscoelastic WLMs rapidly transforms into a flowing water-like solution (BSeUSBe-SDS-Ox, Figure 1b) in no more than 14 min (Figure S10), indicative of a fast redox-induced response. The BSeUSBe-SDS-Ox is a typical Newtonian fluid with approximately constant viscosity of  $\sim 0.001 \text{ Pa}\cdot\text{s}$ , very close to that of water, and their moduli are close to zero, beyond the detection limit of the instrument. Moreover, the viscoelasticity decay time could be remarkably shortened when increasing the amount of  $\text{H}_2\text{O}_2$ . Instead, if further introducing equimolar VC, the viscoelasticity of BSeUSBe-SDS could be easily re-obtained in less than 10 min (BSeUSBe-SDS-Re, Figure 1c), and its flow curve almost completely overlaps with that of BSeUSBe-SDS (Figure 2a), suggesting that the redox-responsiveness is reversible. Just as shown in Figure 2b, BSeUSBe-SDS was reversibly changed between viscoelastic WLMs-gel and low-viscosity solution upon

alternate addition of  $\text{H}_2\text{O}_2$  and VC, without any deterioration after several cycles of repeat. Individually, however, a 50 mM SDS or BSeUSBe brine solution demonstrates water-like fluid behavior either before or after oxidation (Figure S11), and is composed of small spherical micelles with radius of 2.21 nm or 2.40 nm (Figure S12), respectively. This means the WLMs-based gel results from the cooperative self-assembly of BSeUSBe and SDS in brine solution.

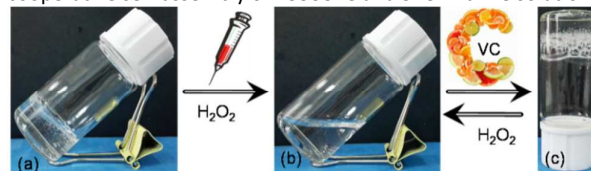


**Figure 1.** Snapshots of redox switchable viscoelastic wormlike micellar system based on 50 mM BSeUSBe-SDS in 50 mM NaCl solution. (a) Initially, the sample appears to be viscoelastic gel; (b) after addition of equimolar  $\text{H}_2\text{O}_2$ , it is highly flowable in no more than 14 min; (c) after addition of VC in the sample b, it re-exhibits gel-like behaviour in 10 min.

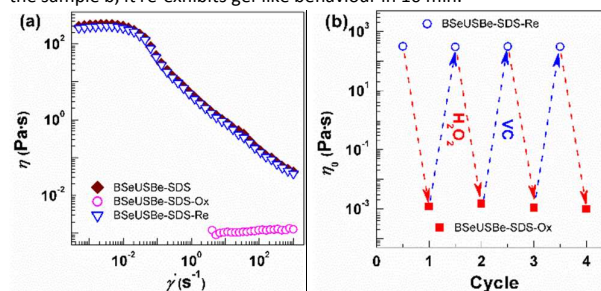


**Figure 2.** Evidence for reversible redox response of viscoelastic surfactant gel. (a) Steady-state rheology, and (b) Reversible change of zero-shear viscosity ( $\eta_0$ ) of the 50 mM BSeUSBe-SDS brine solution with alternate addition of  $\text{H}_2\text{O}_2/\text{VC}$ .

To further corroborate the macroscopic behaviors, FF-TEM observation of microstructures, size measurement by dynamic light scattering (DLS) and small angle X-ray scattering (SAXS) were performed. Before oxidation, dense network-like aggregate formed by flexible elongated random linear aggregates were clearly evidenced in BSeUSBe-SDS (Figures 3a). These threadlike aggregates have diameter of several nanometers and length in the micrometer range, and the mesh size of network is about 22 nm estimated from the DLS results (Figure S13). When  $\text{H}_2\text{O}_2$  is added, big vesicle with a radius of about 100 nm was found (Figure 3b), which also matches exactly the result obtained from the DLS data (Figure S13). Alternately, when VC is added, network-like entanglement of WLMs emerges again in the sample (Figures 3c), replacing vesicles, and the aggregates size also returns back to the initial value (Figure S13). Additionally, the results obtained from the SAXS measurement also confirm the reversible trigger of aggregates structures (Figure S14 and S15). Therefore, the refreshing gel/sol transition observed in BSeUSBe-SDS solution can clearly be ascribed to the evolution of self-organized assemblies from an entangled network of worms to vesicles.

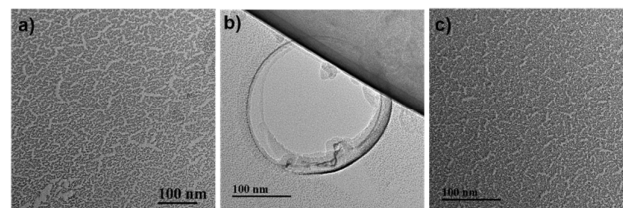


**Figure 3.** Freeze-fracture transmission electron microscopy (FF-TEM) images of redox-triggered wormlike micelles. (a) 50 mM BSeUSBe-SDS before

oxidation; (b) 50 mM BSeUSBe-SDS-Ox (after oxidation) and (c) 50 mM BSeUSBe-SDS-Re (after reduction).

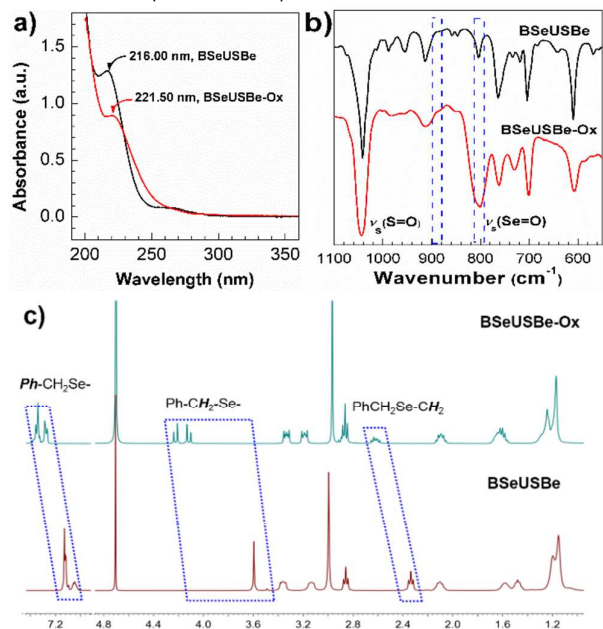


**Figure 4.** Evidences at the molecular level for the redox response of BSeUSBe. (a) UV-vis spectra of 0.1 mM BSeUSBe before and after the addition of  $\text{H}_2\text{O}_2$ . (b) FT-IR spectra of BSeUSBe in absent and present of  $\text{H}_2\text{O}_2$ . (c)  $^1\text{H}$  NMR spectra of BSeUSBe and BSeUSBe-Ox using  $\text{D}_2\text{O}$  as solvent.

Why the same solution shows such different macroscopic rheological behaviors and microscopic aggregates structures in the absence and presence of  $\text{H}_2\text{O}_2$ . Among the species of SDS, BSeUSBe, NaCl and water molecules, only selenium atom of BSeUSBe is redox sensitive to reactive oxygen species released from  $\text{H}_2\text{O}_2$ . We deduce that the above reversible sol/gel transition of BSeUSBe-SDS solution is caused by the different molecular species of the BSeUSBe before and after oxidation, which is the chemical reason for the self-assembly leading to formation of WLMs and vesicles. To confirm this hypothesis, additional mechanistic understanding at the molecular level was thus sought using UV-vis, FT-IR,  $^1\text{H}$  NMR and ESI-MS spectroscopic measurements. As shown in Figure 4a, before oxidation, BSeUSBe solution shows a maximal absorbance  $\lambda_{\text{max}}$  at 216 nm, corresponding to  $\pi$ - $\pi$  conjugate interaction of aromatic ring; after adding equimolar  $\text{H}_2\text{O}_2$ , the  $\lambda_{\text{max}}$  shifted to 221.5 nm, which could be clearly attributed to the strong  $\pi$ - $\pi^*$  conjugate interaction between the C=C in aromatic ring and Se=O, pointing to the oxidation of BSeUSBe. Noteworthy such a red shift ( $\sim 5.5$  nm) is very close to that of increasing an exocyclic double bond,<sup>15</sup> suggesting that the oxidation product is selenoxide, not selenone. Compared with BSeUSBe, after oxidation the characteristic absorption FT-IR bond at  $804\text{ cm}^{-1}$  corresponding to stretching vibration of the Se=O group<sup>11a,16</sup> has an evident increase using the symmetric stretching vibration of the S=O group ( $1042\text{ cm}^{-1}$ ) as a reference, and no bimodal peak can be observed in  $880\text{--}900\text{ cm}^{-1}$  (Figure 4b), both of which also confirm that the formation of selenoxide, not selenone.<sup>11a,16</sup> Furthermore, when exposing to  $\text{H}_2\text{O}_2$ , the signals of the protons neighboring the selenium atom (Ph- $\text{CH}_2$ -Se-, Ph- $\text{CH}_2$ -Se- and Ph- $\text{CH}_2$ -Se- $\text{CH}_2$ ) shift obviously downfield in  $^1\text{H}$  NMR spectrum (Figure 4c), revealing the oxidation of selenium atom. In particular, the peak assigned to Ph- $\text{CH}_2$ -Se- splits into two doublets, which is characteristic of the formation of selenoxide group in Ph $\text{CH}_2$ Se=O. Because the introduction of one oxygen atom

onto the selenium atom, the free rotation of the Ph-C and C-Se bonds was limited, resulting in geminal coupling of Ph $\text{CH}_2$ Se=O, i.e., the selenium atom with asymmetry. Similarly, the peak for Ph- $\text{CH}_2$ -Se- $\text{CH}_2$  also splits due to the geminal  $^2J$  coupling, but one of two doublets overlaps with that of  $-\text{N}^+(\text{CH}_3)_2\text{-CH}_2^-$ . These results in  $^1\text{H}$  NMR spectra also strongly supports the presence of the selenoxide group. Additionally, the ESI-MS results (Figure S16) show that the molecular ion peak of BSeUSBe increases from  $492.3\text{ (MH}^+)$  to  $508.2\text{ (MH}^+)$  or  $530.2\text{ (MNa}^+)$  after addition of  $\text{H}_2\text{O}_2$ , implying that only one oxygen atom was added to the selenium, thus also providing a selenoxide structure. In a word, BSeUSBe is therefore a redox responsive surfactant, in which the selenide was converted to selenoxide after oxidation, resulting in changes in geometrical structure and interfacial properties of BSeUSBe accompanied by an increase of critical micellar concentration (*cmc*) from  $0.30\text{ mM}$  to  $0.92\text{ mM}$  (Figure S17).

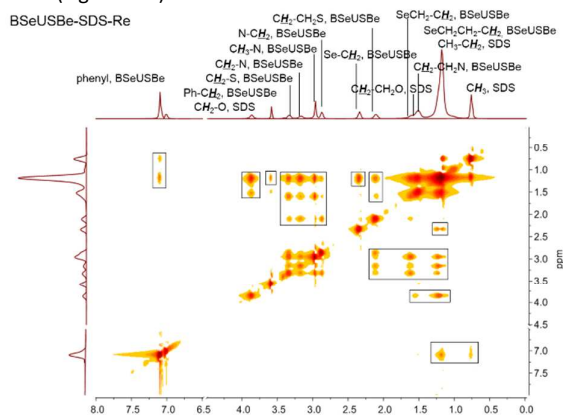


**Figure 5.** 2D NOESY NMR spectra of BSeUSBe-SDS before oxidation.

Additionally, the 2D NOESY NMR spectra (Figure 5) indicates significant positive cross peaks for BSeUSBe-SDS, in which a few prominent intramolecular cross peaks (highlighted in the boxed rectangles) are observed. Through careful analysis of these cross peaks, one can pinpoint that the interaction sites of BSeUSBe and SDS molecules not only exist between the terminal phenyl, Ph- $\text{CH}_2$  protons of BSeUSBe tail and the methyl, methylene protons of SDS tail (Scheme 1), but also present between the  $\text{CH}_2$ - $\text{CH}_2$ -N,  $\text{CH}_2$ -N,  $\text{CH}_3$ -N, N- $\text{CH}_2$  protons of BSeUSBe and the  $\text{CH}_2$ - $\text{CH}_2$ -O,  $\text{CH}_2$ -O protons of SDS. When exposed to  $\text{H}_2\text{O}_2$ , the 2D NOESY NMR spectra (Figure S19) reveals more feeble positive cross peaks compared with BSeUSBe-SDS. Of special importance is that the cross peaks related to the terminal phenyl, Ph- $\text{CH}_2$  protons of BSeUSBe tail almost disappears from the spectra. Furthermore, many pre-existing intramolecular interaction cross peaks also evidently weaken, and even die away. These mean that the hydrophobic tail of BSeUSBe should be still located in the hydrophobic micelles core (Scheme 1), but the distance to the tail of SDS becomes too long to bring the same intramolecular interaction as that of before oxidation. On the other side, no matter before or after oxidation, all the protons signals of BSeUSBe-SDS do not show any shift compared with those of single BSeUSBe or SDS (Figure S20 and S21). This further confirm that the micro-environment of all the protons almost remains constant before and after mixing BSeUSBe and SDS, both for oxidative and reductive states.

In light of the results discussed above, the following mechanism is proposed to account for the “on” and “off” switching of the novel WLMs (Scheme 1). It is well known that drastic changes in rheological properties correlate with changes in the microstructure of the aggregates, which can broadly be discussed based on the

packing parameter,  $P = u/al$ ,<sup>17</sup> where  $a$  is the effective headgroup area and  $u$  the volume of the lipophilic chain possessing a maximum effective length  $l$ . For  $P < 1/3$ , spherical micelles are formed; for  $1/3 < P < 1/2$ , cylindrical and WLMs are found while  $1/2 < P < 1$  lead to vesicles or bilayers.

Similar to SDS, BSeUSBe in diluted NaCl solution only self-assemble into some small globular aggregates (Figure S12) due to a small  $u$ , showing high fluidity. When SDS is added into the solution, BSeUSBe can provide a positively charge site, quaternary ammonium ion, to link noncovalently one SDS molecules with negative charge by electrostatic attraction forming a pseudo "hanger" type structure: one hydrophilic head and two hydrophobic tails (Scheme 1). Due to the strong intramolecular hydrophobic interaction originated from two tails of BSeUSBe and SDS (Figure 5), this pseudo "hanger" type surfactant possesses a lower  $cmc$ , 0.10 mM (Figure S18), which is far below that of single SDS<sup>7c</sup> or BSeUSBe (0.30 mM), indicative of the strong self-assemble ability. Moreover, two hydrophobic tails in BSeUSBe-SDS brings an great increase of the parameter  $u$ , making the  $P$  more readily locating in the range of  $1/2 \sim 1/3$ , aggregating into long WLMs.<sup>17</sup> These flexible WLMs entangle with each other into a 3D network, reminiscent of polymer solutions, remarkably enhancing the viscoelasticity of the solutions, behaving gel-like. In fact, this model is consistent with the observed macroscopic viscoelastic response and microscopic micellar morphology of BSeUSBe-SDS.

Upon treatment with H<sub>2</sub>O<sub>2</sub>, original hydrophobic selenide in BSeUSBe turns into less hydrophobic selenoxide, leading to an evident increase in  $cmc$ , 0.45 mM for BSeUSBe-SDS-Ox (Figure S18), more than 4 times of that of BSeUSBe-SDS. Namely, the self-assemble ability drops. Nevertheless, the hydrogen interaction of the Se=O group does not cause the hydrophobic tail of BSeUSBe-Ox to flee the hydrophobic micellar cores. In the fact, the 2D NOESY NMR (Figure S19) and <sup>1</sup>H NMR spectra (Figure S21) has demonstrated that the hydrophobic tail of BSeUSBe-Ox is still in the hydrophobic micellar cores, but the distance between the hydrophobic tails of BSeUSBe-Ox and SDS begins to getting longer than that of reductive state. That is say the BSeUSBe tail tends to remove away from SDS tail. Thus, the volume  $u$  of the lipophilic chain is further swelled, leading to a deviation of the  $P$  from the range of  $1/2 \sim 1/3$  to  $1/2 \sim 1$ , which favors the formation of vesicles or bilayers,<sup>17</sup> leading to a drop in the viscosity. The rheological data and FF-TEM observation fully verify the deduction. The sample however is able to immediately recover its initial WLMs-based network and packing if VC is added again, because of the reduction of selenoxide to selenide, and thus the solution re-appears high viscoelasticity. Therefore, the reversible macroscopic response of BSeUSBe-SDS in reductive and oxidative states can be ascribed to the change of the microscopic morphology of self-organized aggregates originating from the variation of intramolecular interaction of BSeUSBe and SDS.

In summary, a novel redox-control reversible WLMs based on coassembly of selenium-containing BSeUSBe, and commercially available SDS, in brine solution was developed, reflecting the revolution of microscopic morphology from viscoelastic worms to low viscosity vesicles. Compared with ferrocenyl surfactant-based WLMs, the present system exhibits a faster, more sensitive rheological response, and the morphology smart transforms from worms to vesicles other than short rodlike micelles. These unique features may open up the prospect of using selenium atom as redox-responsive locus to selectively thicken and separate specific fluids, providing potential application as a smart gel in the fields of GPx mimic,<sup>9</sup> encapsulation and localization of bioactive molecules

and cells in the gel matrix.<sup>18</sup> For example, we have demonstrated that the GPx catalytic activity of BSeUSBe-SDS WLMs is very low; while the vesicles transformed from the WLMs upon the oxidation of H<sub>2</sub>O<sub>2</sub>, show extremely high GPx activity (Figure S22). The mechanism of controlling catalytic activity are being investigated, and will be reported elsewhere soon.

## Acknowledge

This work is financially supported by the MOE & SAFEA for the "111 Project" (B13025), the Fundamental Research Funds for the Central Universities (JUSRP11421), the open research fund of Key Laboratory of Food Colloids and Biotechnology Ministry of Education, Jiangnan University (JDSJ2013-08), Qinglan Project of Jiangsu Province, National Natural Science Foundation of China (21173207).

## Notes and references

- 1 a) M. A. C. Stuart, W. T. S. Huck, J. Genzer, M. Muller, C. Ober, M. Stamm, G. B. Sukhorukov, I. Szleifer, V. V. Tsukruk, M. Urban, F. Winnik, S. Zauscher, I. Luzinov and S. Minko, *Nat. Mater.*, 2010, **9**, 101; b) M. J. Solomon, *Nature*, 2010, **464**, 496–498.
- 2 a) Z. Chu, C. A. Dreiss and Y. Feng, *Chem. Soc. Rev.*, 2013, **42**, 7174; b) J. Eastoe and A. Vesperinas, *Soft Matter*, 2005, **1**, 338; c) Y. Zhang, Z. Guo, J. Zhang, Y. Feng, B. Wang and J. Wang, *Prog. Chem.*, 2011, **23**, 2012.
- 3 a) H. Hoffmann and G. Ebert, *Angew. Chem. Int. Ed.*, 1988, **27**, 902; b) J. Cardiel, A. C. Dohnalkova, N. Dubash, Y. Zhao, P. Cheung and A. Q. Shen, *Proc. Natl. Acad. Sci. U. S. A.*, 2013, **110**, 1653.
- 4 M. E. Cates, *Macromolecules*, 1987, **20**, 2289.
- 5 a) H. Sakai, Y. Orihara, H. Kodashima, A. Matsumura, T. Ohkubo, K. Tsuchiya and M. Abe, *J. Am. Chem. Soc.*, 2005, **127**, 13454; b) H. Y. Lee, K. K. Diehn, K. S. Sun, T. H. Chen and S. R. Raghavan, *J. Am. Chem. Soc.*, 2011, **133**, 8461; c) Y. Lin, X. Cheng, Y. Qiao, C. Yu, Z. Li, Y. Yan and J. Huang, *Soft Matter*, 2010, **6**, 902.
- 6 a) T. S. Davies, A. M. Ketner and S. R. Raghavan, *J. Am. Chem. Soc.*, 2006, **128**, 6669; b) Z. Chu and Y. Feng, *Chem. Commun.*, 2011, **47**, 7191.
- 7 a) Y. Zhang, Y. Feng, J. Wang, S. He, Z. Guo, Z. Chu, C. A. Dreiss, *Chem. Commun.*, 2013, **49**, 4902; b) Y. Zhang, Z. Chu, C. A. Dreiss, Y. Wang, C. Fei and Y. Feng, *Soft Matter*, 2013, **9**, 6217; c) Y. Zhang, Y. Feng, Y. Wang and X. Li, *Langmuir*, 2013, **29**, 4187; d) X. Su, M. F. Cunningham and P. G. Jessop, *Chem. Commun.*, 2013, **49**, 2655; e) Y. Zhang and Y. Feng, *J. Colloid Interface Sci.*, 2015, **447**, 173; f) Y. Zhang, P. An, X. Liu, Y. Fan and X. Hu, *Colloid Polym. Sci.*, 2015, **293**, 357.
- 8 a) Y. Zhang, Y. Han, Z. Chu, S. He, J. Zhang and Y. Feng, *J. Colloid Interface Sci.*, 2013, **394**, 319; b) Y. Lin, X. Han, J. Huang, H. Fu and C. Yu, *J. Colloid Interf. Sci.*, 2009, **330**, 449; c) Y. Zhang, P. An and X. Liu, *Soft Matter*, 2015, **11**, 2080.
- 9 a) H. Xu, W. Cao and X. Zhang, *Accounts Chem. Res.*, 2013, **46**, 1647; b) R. Boyd, *Nat. Chem.*, 2011, **3**, 570; c) X. Huang, X. Liu, Q. Luo, J. Liu and J. Shen, *Chem. Soc. Rev.*, 2011, **40**, 1171.
- 10 K. Tsuchiya, Y. Orihara, Y. Kondo, N. Yoshino, T. Ohkubo, H. Sakai and M. Abe, *J. Am. Chem. Soc.*, 2004, **126**, 12282.
- 11 a) T. Wirth, *Organoselenium chemistry: Synthesis and reactions*; Wiley-VCH Verlag GmbH & Co. KgaA, Weinheim, Germany, 2012; b) S. Ji, W. Cao, Y. Yu and H. Xu, *Angew. Chem. Int. Ed.*, 2014, **53**, 6781.
- 12 H. Hoffmann, in *Structure and flow in surfactant solutions*, American Chemical Society, Washington, DC, 1994.
- 13 R. Kumar, G. C. Kalur, L. Ziserman, D. Danino and S. R. Raghavan, *Langmuir*, 2007, **23**, 12849.

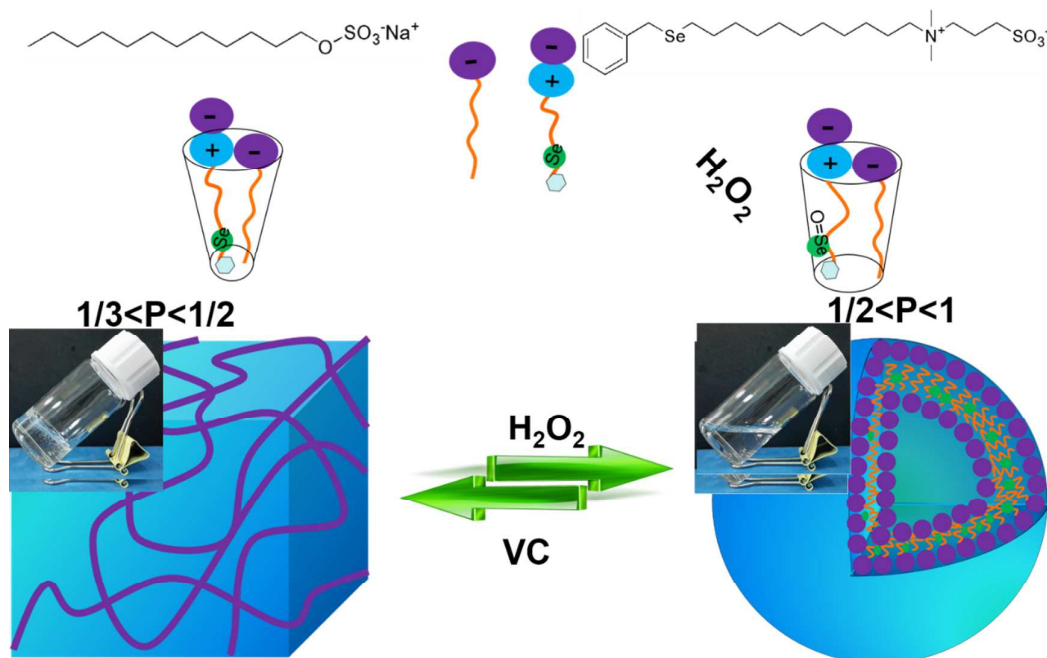
Journal Name

COMMUNICATION

- 14 P. G. de Gennes, Scaling concepts in polymer physics; Cornell University Press, Ithaca, New York, 1979.
- 15 E. Pretsch, P. Buhlmann and C. Affolter, Structure determination of organic compounds; Springer-Verlag Berlin and Heidelberg GmbH & Co. K, New York, 2009.
- 16 G. Socrates, Sulphur and selenium compounds: Infrared characteristic group frequencies; John Wiley & Sons: New York, 1980, Chapter 16.
- 17 J. N. Israelachvili, D. J. Mitchell and B. W. Ninham, *J. Chem. Soc., Faraday Trans. II*, 1976, **272**, 1525.
- 18 F. Peng, G. Li, X. Liu, S. Wu and Z. Tong, *J. Am. Chem. Soc.*, 2008, **130**, 16166.

## Switching wormlike micelles of selenium-containing surfactant using redox reaction\*\*

Yongmin Zhang,<sup>a\*</sup> Weiwei Kong,<sup>a</sup> Cheng Wang,<sup>a</sup> Pengyun An,<sup>a</sup> Yun Fang,<sup>a</sup> Zhirong Qin,<sup>c</sup> Yujun Feng,<sup>\*b</sup> Xuefeng Liu<sup>\*a</sup>



Wormlike micelles based on selenium-containing surfactant and commercially anionic surfactant reversibly response to  $H_2O_2$  and vitamin C, and show circulatory gel/sol transition, reflecting changes in aggregate morphology from entangled worms to vesicles.